Arch Toxicol (2011) 85:1057–1065
DOI 10.1007/s00204-011-0645-x

MOLECULAR TOXICOLOGY

Ceramide induces apoptosis via caspase-dependent and caspase-independent pathways in mesenchymal stem cells derived from human adipose tissue

Ji Yeon Park · Moon Jung Kim · Yong Keun Kim · Jae Suk Woo

Received: 8 April 2010 / Accepted: 6 January 2011 / Published online: 23 January 2011

Abstract Apoptosis of stem cells may be related to certain degenerative conditions such as progressive tissue damage and an inability to repair. Ceramide induces cell death in various cell types. However, the underlying mechanisms of ceramide-induced cell death in stem cells are not explored. This study was designed to investigate the cell death process caused by cell-permeable ceramide and to determine the underlying mechanisms in mesenchymal stem cells derived from human adipose tissue (hASCs). Ceramide caused a loss of cell viability in a concentration- and time-dependent manner, which was largely attributable to apoptosis. Ceramide induced generation of reactive oxygen species (ROS) and disruption of the mitochondrial membrane potential. The ROS generation caused by ceramide was prevented by the antioxidant *N*-acetylcysteine (NAC). Although ceramide induced release of cytochrome c from mitochondria and activation of caspase-3, the ceramide-induced cell death was partially prevented by caspase inhibitors. Addition of ceramide caused apoptosis-inducing factor (AIF) nuclear translocation, which was prevented by antioxidant. Taken together, these data suggest that ceramide induces cell death through both caspase-dependent and caspase-independent mechanisms mediated by ROS generation in hASCs.

J. Y. Park · M. J. Kim · Y. K. Kim · J. S. Woo (✉)
Department of Physiology, Pusan National University School of Medicine, Gyeongsangnam-do, Yangsan 626-870, Korea
e-mail: jswoo@pusan.ac.kr

J. Y. Park · J. S. Woo
BK21 Medical Science Education Center, Gyeongsangnam-do, Yangsan 626-870, Korea

Keywords Ceramide · Apoptosis · Reactive oxygen species · Caspase · Apoptosis-inducing factor · Mesenchymal stem cells derived from human adipose tissue

Introduction

Ceramide has been implicated in numerous cellular processes, including cell proliferation, cell cycle arrest, differentiation, and apoptosis (Futerman and Hannun 2004). Ceramide can be released from the cell membrane by enzymes and subsequently acts as a signaling molecule (Colombaini and Garcia-Gil 2004). In other words, exogenous cell-permeable ceramide and endogenous ceramide generated by sphingomyelinase activation can lead to apoptosis in many different cell types (Hannun and Obeid 2002), indicating that ceramide acts as a mediator of apoptosis (Cuvillier 2002). Ceramide is generated and accumulated under various conditions such as apoptotic stimulus, environmental stress, and chemotherapeutic agent (Woodcock 2006).

Human mesenchymal stem cells (MSCs) are multipotent and can be separated from bone marrow, periosteum, cord blood, skeletal muscle, and adipose tissue (Barry and Murphy 2004). MSCs have self-renewal capacity and the potential to differentiate into cell types of the mesodermal lineage such as adipocytes, osteocytes, chondrocytes, and myocytes (Short et al. 2003). Mesenchymal stem cells derived from human adipose tissue (hASCs) have been shown to have similar differentiation potential to bone marrow-derived mesenchymal stem cells (BMSCs; De Ugarte et al. 2003). Although the proliferation and differentiation of MSCs have been widely studied (Jeon et al. 2005; Kim et al. 2006), little information is available on the

underlying mechanism of apoptosis in MSCs. Depletion or functional alterations of MSCs may be associated with certain degenerative conditions such as progressive tissue damage and an inability to repair damaged tissues (Barry and Murphy 2004). Indeed, it was found that the proliferative capacity of MSCs was reduced in patients with osteoarthritis (Murphy et al. 2002) and osteoporotic patients (Rodríguez et al. 2004).

Although ceramide inhibits differentiation and induces apoptosis of stem cells (Bieberich et al. 2003, 2004), the underlying mechanism remains unclear. Therefore, the present study was undertaken to examine the effects of ceramide on cell death and to determine the underlying mechanisms in mesenchymal stem cells derived from human adipose tissue (hASCs). The present study indicated that ceramide induced apoptosis through caspase activation and AIF nuclear translocation mediated by ROS generation.

Materials and methods

Reagents

C_2-ceramide, propidium iodide, Hoechst 33258, 3-[4,5-dimethylthiazol2-yl]-2,5-diphenyltetrazolium bromide (MTT), and *N*-acetylcysteine (NAC) were purchased from Sigma–Aldrich Chemical (St. Louis, MO, USA). Tween 20, Z-VAD-FMK, and DEVD-CHO were purchased from Calbiochem (La Jolla, CA, USA). 3,3′-Dihexyloxacarbocyamide [$DiOC_6$] and 2,7-dichlorofluorescein diacetate (DCFH-DA) were purchased from Molecular Probes (Eugene, OR, USA). FITC Annexin V Apoptosis Detection Kit was purchased from BD Biosciences (San Jose, CA, USA). NucView™ 488 Caspase-3 Assay Kit for Live Cells was purchased from Biotium, Inc. (Hayward, CA, USA). The anti-cytochrome c antibody was purchased from Santa Cruz Biotechnology, Inc. (Santa Cruz, CA, USA). The anti-AIF and anti-α-actin antibodies were purchased from Cell Signaling Technology, Inc. (Beverly, MA, USA). Horseradish peroxidase-conjugated secondary antibodies were purchased from Jackson ImmunoResearch Laboratories (West Grove, PA, USA). All other chemicals were of the highest commercial grade available.

Cell culture

Subcutaneous adipose tissue was obtained from consenting Korean patients undergoing elective surgeries, and all protocols were approved by the Institutional Review Board of Pusan National University (Lee et al. 2004). Mesenchymal stem cells from adipose tissues were prepared from 3 different patients (4-, 10-, and 11-year-old males). Briefly, liposuction tissue was washed with Hank's balanced salt solution (HBSS) at least three times and then digested with 0.075% type I collagenase for 30 min at 37°C. The enzyme activity was neutralized by minimum essential medium alpha (α-MEM, Gibco. Invitrogen Co., CA, USA) containing 10% fetal bovine serum (FBS, Hyclone, UT, USA), and the samples were centrifuged for 10 min at 1,200×*g*. The cell pellet was resuspended in culture medium (α-MEM, 10% FBS, 100 units/ml penicillin, and 100 μg/ml streptomycin) and plated in tissue culture dishes at 3,500 cells/cm^2 for 24 h at 37°C in a humidified atmosphere of 95% air and 5% CO_2. After 24 h, nonattached cells were removed, and the tissue culture plate was washed. The primary hASCs were cultured for 5–7 days until they reached confluence and were defined as passage "0". We used 3–10 passage number of hASCs in this study. In each experiment, the cells seeded at a density of 5×10^4 cells/well in 24-well plates or 2×10^5 cells/well in 6-well plates and incubated in culture medium for 24 h at 37°C in a humidified atmosphere of 95% air and 5% CO_2.

Measurement of cell viability and cell death

Cell viability was determined using an MTT assay (Denizot and Lang 1986). Cells (5×10^4 cells/well) were seeded in 24-well plates with culture medium and the experiment was performed 2 days after seeding. The cells were treated with ceramide of various concentrations for 24 h or with 50 μM ceramide for various times. After washing the cells with HBSS, culture medium containing 0.5 mg/ml MTT was added to each well. The cells were incubated for 2 h at 37°C, and the supernatant was then removed. The viable cells formed formazan crystals that were solubilized with 0.2 ml of dimethyl sulfoxide (DMSO). A 0.1-ml aliquot of each sample was then transferred to 96-well plates, and the absorbance of each well was measured at 570 nm using an ELISA reader (FLUOstarOPTIMA, *BMG LABTECH*, Offenburg, Germany). The data were expressed as a percentage of the control measured in the absence of ceramide.

Cell death was evaluated using a trypan blue exclusion assay. The cells were seeded and treated as described earlier. After washing the cells with HBSS, cells were harvested with 0.025% trypsin and dyed with a 0.4% trypan blue solution. The number of viable and nonviable cells was counted using a hemocytometer under a light microscope. Cells failing to exclude the dye were considered to be nonviable.

Measurement of apoptosis

Apoptosis was estimated using an FITC Annexin V Apoptosis Detection Kit (BD Biosciences, San Jose, CA, USA) and flow cytometric analysis (FACSCalibur™ and

CellQuest™, Beckton Dickinson, Franklin Lakes, NJ, USA).

The annexin V binding assay was performed as described in the manufacturer's manual. Cells (2×10^5 cells/well) were seeded in 6-well plates with culture medium and the experiment was performed 2 days after seeding. The cells were treated with 50 μM ceramide for 24 h in serum-free culture medium. Cells were harvested with 0.025% trypsin and washed with cold PBS and then resuspended in annexin V binding buffer. The cells were then incubated for 15 min with binding solution containing FITC annexin V and propidium iodide in the dark and measured by flow cytometric analysis with the excitation filter at 488 nm. The percentage of apoptotic cells was calculated as the quadrant statistics of the early and late apoptotic region to the entire cell population (1×10^4 cells).

For cell cycle assay, the cells were seeded and treated with 50 μM ceramide as described previously. The floating cells and adherent cells with 0.025% trypsin treatment were harvested. The pellet was washed with cold PBS, centrifuged again and fixed with cold 70% ethanol containing 0.5% Tween 20 for 24 h at 4°C. The pellet was then washed with cold PBS, resuspended in 1.0 ml of propidium iodide solution (50 μg/ml propidium iodide, 100 μg/ml RNase) and incubated for 30 min at 37°C. Apoptotic cells were measured as described earlier. Cells with sub-G_1 propidium iodide incorporation were considered to be apoptotic. The percentage of apoptotic cells was calculated as the histogram statistics of the sub-G_1 cells to the entire cell population.

Measurement of reactive oxygen species

The intracellular generation of reactive oxygen species (ROS) was measured using DCFH-DA. This nonfluorescent ester enters into cells and is hydrolyzed to DCFH by cellular esterases. The DCFH probe is rapidly oxidized to the highly fluorescent molecule 2,7-dichlorofluorescein (DCF) in the presence of cellular peroxidase and ROS such as hydrogen peroxide or fatty acid peroxides. Cells (2×10^5 cells/well) were seeded in 6-well plates with culture medium, and the experiment was performed 2 days after seeding. The cells were preincubated in serum-free culture medium with 30 μM DCFH-DA for 1 h at 37°C. After preincubation, the cells were treated with 50 μM ceramide for various times. Changes in DCF fluorescence were measured by flow cytometric analysis (FACSCalibur™ and CellQuest™, Beckton Dickinson, Franklin Lakes, NJ, USA) with the excitation filter at 488 nm. Effect of antioxidant NAC on the ceramide-induced cell death was determined using an MTT assay. Cells (5×10^4 cells/well) were seeded in 24-well plates with culture medium, and the experiment was performed 2 days after seeding. The cells were preincubated with antioxidant NAC for 15 min and then treated with 50 μM ceramide.

Measurement of the mitochondrial membrane potential

The value of mitochondrial membrane potential ($\Delta\Psi m$) was measured by $DiOC_6(3)$, a green fluorescent membrane dye that is incorporated into cells depending upon the $\Delta\Psi m$ (Pastorino et al. 1998). Cells (2×10^5 cells/well) were seeded in 6-well plates with culture medium, and the experiment was performed 2 days after seeding. The cells were treated with 50 μM ceramide for various times. The loss of $DiOC_6(3)$ fluorescence indicates disruption of the mitochondrial inner transmembrane potential. Cells were stained with 50 nM $DiOC_6(3)$ for 20 min at 37°C in the dark. They were then washed and resuspended in HBSS containing Ca^{2+} and Mg^{2+}. The fluorescence intensity was measured by flow cytometric analysis (FACSCalibur™ and CellQuest™, Beckton Dickinson, Franklin Lakes, NJ, USA) with the excitation filter at 488 nm.

Measurement of cytochrome c release and caspase-3 activity

The release of cytochrome c from the mitochondria into the cytosol was measured by Western blot analysis (Rosse et al. 1998). Cells (2×10^5 cells/well) were seeded in 6-well plates with culture medium, and the experiment was performed 2 days after seeding. The cells were incubated with 50 μM ceramide in serum-free culture medium for various times. Cells were harvested each duration, washed with HBSS and incubated with extraction buffer (10 mM HEPES, 250 mM sucrose, 10 mM KCl, 1.5 mM $MgCl_2$, 1 mM EDTA, 0.05% digitonin, and 1 mM phenylmethylsulfonyl fluoride) for 10 min at 4°C. They were then centrifuged at $100{,}000 \times g$ for 15 min at 4°C, and the supernatant containing cytosolic fraction (protein 10–20 μg) was transferred into a new tube. The cell pellet was incubated with lysis buffer (1% Triton X-100, 1 mM EGTA, 1 mM EDTA, 10 mM Tris–HCl, pH 7.4, and protease inhibitors) for 10 min at 4°C and centrifuged at $100{,}000 \times g$ for 15 min at 4°C. The supernatant containing mitochondrial fraction (protein 5–10 μg) was transferred to a new tube. Protein (5–10 μg) of each fraction was loaded on a 12% SDS–polyacrylamide gel and later transferred onto a nitrocellulose membrane. The membrane was blocked with 5% skim milk for 30 min at room temperature and probed with a rabbit polyclonal anti-cytochrome c primary antibody (dilution 1:1,000), followed by a horseradish peroxidase-conjugated secondary antibody (dilution 1:2,500). The signal was visualized using an enhanced chemiluminescence (Amersham, Buckinghamshire, UK) with X-ray film.

Caspase-3 activity was measured using the NucView™ 488 Caspase-3 Assay Kit for Live Cells (Biotium, Inc., Hayward, CA, USA), as described in the manufacturer's manual. The cells were seeded and treated with 50 μM ceramide as described earlier. Cells were harvested for each duration with 0.025% trypsin and centrifuged at 250×*g*. The cell pellet was then incubated with binding solution containing 5 μM NucView™ 488 Caspase-3 substrates for 15 min. The fluorescence intensity was measured by flow cytometric analysis (FACSCalibur™ and CellQuest™, Beckton Dickinson, Franklin Lakes, NJ, USA) with the excitation filter at 488 nm.

Measurement of apoptosis-inducing factor nuclear translocation

The nuclear translocation of apoptosis-inducing factor (AIF) was measured by Western blot analysis as described in cytochrome c measurement section. Cells (2×10^5 cells/well) were seeded in 6-well plates with culture medium, and the experiment was performed 2 days after seeding. The cells were incubated with 50 μM ceramide for 24 h in serum-free culture medium. Then, the cells were harvested and washed with HBSS and incubated with extraction buffer. The supernatant represented the cytosolic proteins. Cytosolic proteins were removed, and the pellet was incubated in the nuclear extraction buffer (350 mM NaCl, 1 mM EGTA, 1 mM EDTA, 10 mM Tris–HCl, pH 7.4 and protease inhibitors) for 10 min at 4°C and centrifuged at 100,000×*g* for 15 min at 4°C. The protein (5–10 μg) was loaded on a 12% SDS–polyacrylamide gel and later transferred onto a nitrocellulose membrane. The membrane was blocked with 5% skim milk for 30 min at room temperature and probed with a rabbit polyclonal anti-AIF primary antibody (dilution 1:1,000), followed by a horseradish peroxidase-conjugated secondary antibody (dilution 1:2,500).

For immunocytochemistry, cells (2×10^5 cells/well) were grown on 22-mm glass coverslips in 6-well plates with culture medium, and the experiment was performed 2 days after seeding. The cells were incubated with 50 μM ceramide with and without antioxidant NAC for 24 h in serum-free culture medium. The cells were washed with HBSS, fixed with 4% paraformaldehyde for 15 min at 4°C, permeabilized with 0.5% Triton X-100 for 10 min at room temperature, washed with PBS, and blocked with 8% bovine serum albumin (BSA) in Tris-buffered saline containing with 0.01% Triton X-100 (TBST) for 1 h at room temperature. The cells were then incubated with a rabbit polyclonal anti-AIF primary antibody (dilution 1:500) overnight at 4°C, washed with TBST, and incubated with a FITC-conjugated secondary antibody (dilution 1:1,000) (Jackson ImmunoResearch Laboratories, PA, USA) for 1 h at room temperature. Nuclei were counterstained with 10 μM Hoechst 33258 to determine AIF nuclear localization. The cells were washed and visualized using a confocal microscope (Leica, Wetzlar, Germany).

Statistical analysis

The data are expressed as the mean ± SEM, and the difference between two groups was evaluated by unpaired Student's *t* test. Multiple group comparison was done using one-way analysis of variance followed by the Tukey post hoc test using SPSS v10.1 (SPSS Inc., Chicago, IL, USA). A probability level of 0.05 was used to establish significance.

Results

Effect of ceramide on cell viability

To estimate the effect of ceramide on the viability of hASCs, the cells were treated with various concentrations of ceramide for 24 h, and the viability was determined using an MTT assay. Ceramide decreased cell viability in a concentration- and time-dependent manner (Fig. 1a and b). Similar results were also obtained by the trypan blue exclusion assay (Fig. 1c and d), indicating that reduction in cell viability was attributed to cell death. To determine whether ceramide induces cell death through apoptosis, cells were treated with 50 μM ceramide for 24 h, and apoptosis was evaluated using an annexin V binding assay and a cell cycle assay. After 24-h incubation, 19.27% of the cells were in an early apoptotic stage (only annexin V positive) and 11.45% were in a later stage of apoptosis (annexin V- and PI positive) as shown in Fig. 2a. To further verify the apoptosis, a flow cytometric analysis was performed in ceramide-treated cells. The sub-G0/G1 peak indicates a population of cells with reduced DNA staining, probably due to DNA fragmentation, and this peak was increased from 3.30% in the control cells to 34.88% in the ceramide-treated cells (Fig. 2b). These data suggest that the cell death caused by ceramide is largely attributed to apoptosis.

Role of ROS in the cytotoxicity of ceramide

To determine whether ceramide induced ROS generation in hASCs, the cells were exposed to ceramide, and changes in DCF fluorescence were measured by flow cytometry. The fluorescence intensity increased about 2.8-fold at 3 h after treatment with ceramide and remained unchanged thereafter up to 24 h (Fig. 3a and b). To determine whether ROS generation was responsible for the ceramide-induced cell death, we evaluated the effect of an antioxidant on the cell death. The cell death induced by ceramide could be

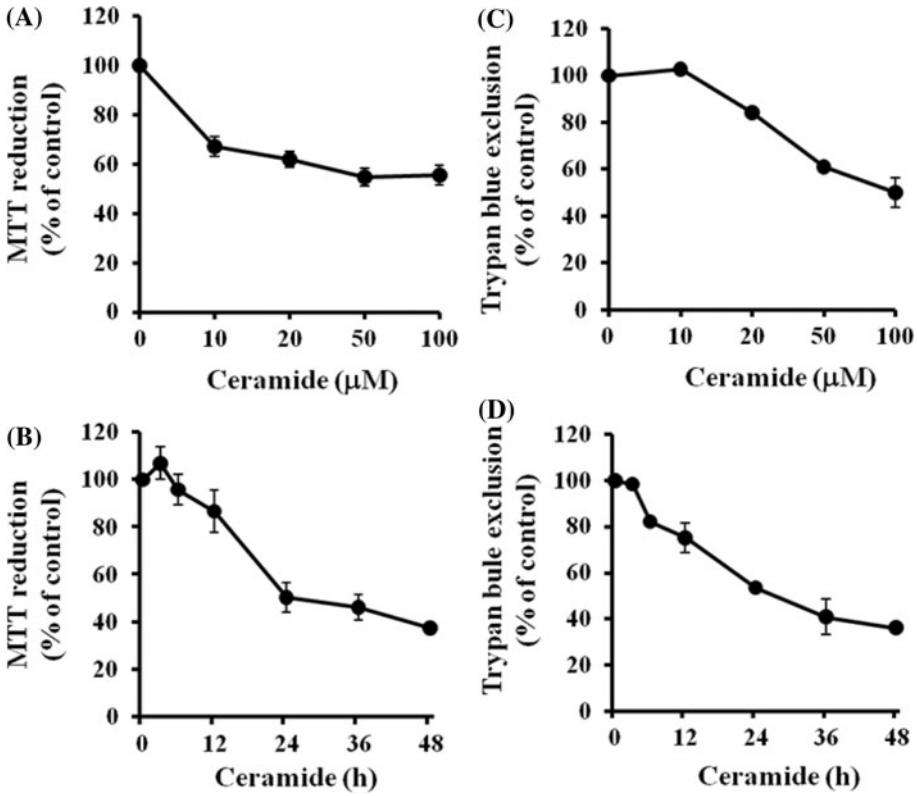

Fig. 1 Effect of ceramide on cell viability. Cell viability was estimated by MTT assay (**a** and **b**) and cell death was measured trypan blue exclusion (**c** and **d**). hASCs were treated with ceramide at the indicated concentrations for 24 h (**a** and **c**) or with 50 μM ceramide for various durations (**b** and **d**). Data are the mean ± SEM of three independent experiments performed in duplicate

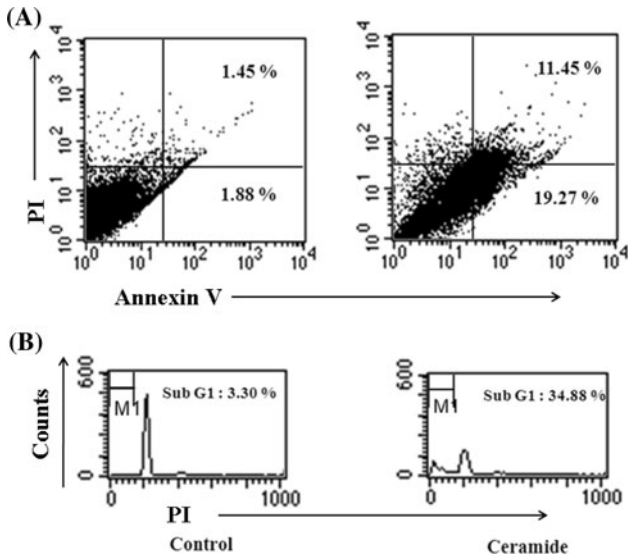

Fig. 2 Induction of apoptosis by ceramide. **a** hASCs were exposed to 50 μM ceramide for 24 h, and apoptosis was estimated by FITC-conjugated annexin V binding assay as described under "Materials and methods". The *numbers* indicate the percentage of cells in each quadrant. Early apoptotic and late apoptotic cells are shown in *right lower* and *right upper* quadrants, respectively. **b** Cells exposed to 50 μM ceramide for 24 h were stained with propidium iodide, and apoptosis was evaluated by flow cytometry. Cells with sub-G_1 propidium iodide incorporation (M1 region) were considered to be apoptotic

prevented by the antioxidant NAC (Fig. 3c), suggesting that ROS generation is involved in ceramide-induced cell death.

Role of mitochondria in ceramide-induced cell death

To determine the role of mitochondria in ceramide-induced cell death, we exposed the cells to ceramide and measured the mitochondrial membrane potential using a fluorescent dye. After treatment with ceramide for 6 h, disruption of the $\Delta\Psi m$ was measured by flow cytometry as evidenced by an increase in the proportion of cells with lower fluorescence intensity and reduction in $\Delta\Psi m$ remained unchanged to 24 h (Fig. 4a and b).

Role of caspase activation in ceramide-induced cell death

Caspase plays a key role in the execution of diverse types of apoptosis (Cohen 1997). To determine whether ceramide induced apoptosis through a caspase-dependent pathway, the cells were exposed to ceramide and changes in cytochrome c in cytosolic and mitochondrial fractions were measured by Western blot analysis. Cytochrome c was released from mitochondria into the cytosol in cells treated with ceramide (Fig. 5a). In addition, ceramide induced

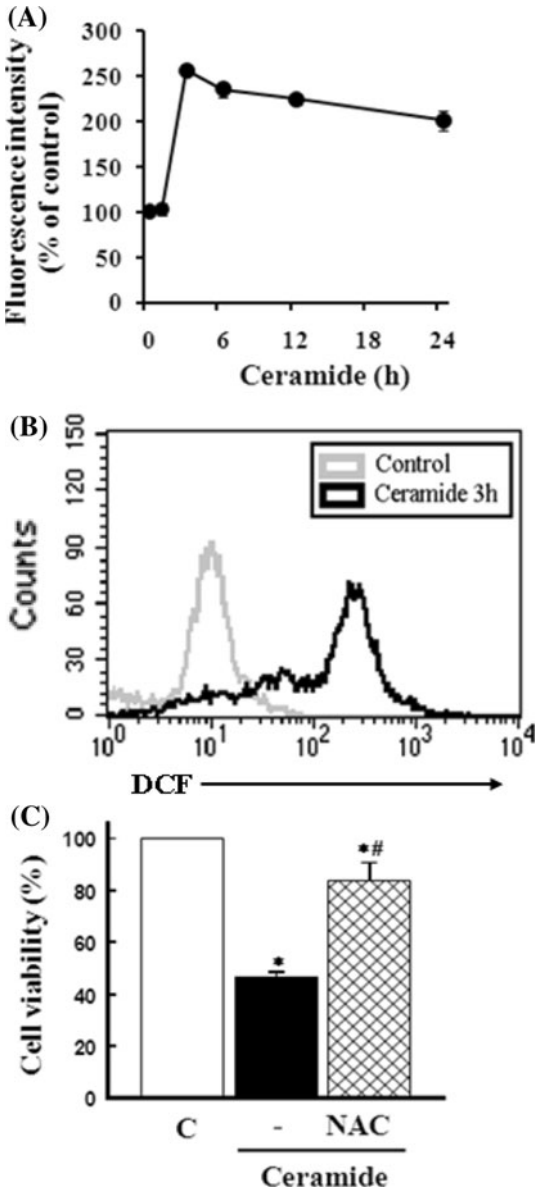

Fig. 3 Effect of ceramide on reactive oxygen species (ROS) generation. ROS was measured by flow cytometric analysis using DCFH-DA. **a** hASCs were treated with 50 μM ceramide for the indicated times. Data are the mean ± SEM of three independent experiments performed in duplicate. **b** Representative tracing of ROS generation at 3 h after ceramide treatment. **c** Effect of antioxidant on ceramide-induced cell death. hASCs were treated with 50 μM ceramide for 24 h in the presence or absence of 1 mM *N*-acetylcysteine (NAC). Cell viability was measured by MTT assay. Data are the mean ± SEM of four independent experiments performed in duplicate. $^{*}P < 0.05$ compared with control; $^{\#}P < 0.05$ compared with ceramide alone

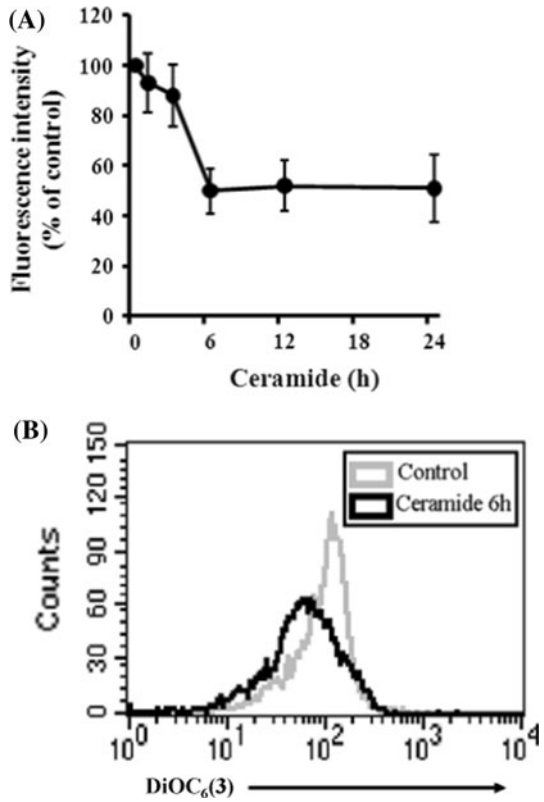

Fig. 4 Effect of ceramide on mitochondrial membrane potential (ΔΨm). The ΔΨm was evaluated by the uptake of the membrane potential-sensitive fluorescent dye $DiCO_6(3)$ as described under "Materials and methods". The fluorescence intensity was analyzed by flow cytometry. **a** hASCs were treated with 50 μM ceramide for the indicated times. Data are the mean ± SEM of three independent experiments performed in duplicate. **b** Representative tracing of changes in ΔΨm at 6 h after ceramide treatment

caspase activation (Fig. 5b), but ceramide-induced cell death was only partially blocked by the general caspase inhibitor, Z-VAD-FMK, and the caspase-3 inhibitor, DEVD-CHO (Fig. 5c), suggesting that ceramide induces cell death through a caspase-dependent and caspase-independent pathway.

The role of AIF nuclear translocation in ceramide-induced cell death

To determine whether AIF nuclear translocation is involved in the ceramide-induced cell death, the effect of ceramide on AIF nuclear translocation was examined by immunocytochemistry and Western blot analysis (Fig. 6a and b). Ceramide induced AIF nuclear translocation at 12 h, but pretreatment with the antioxidant NAC blocked ceramide-induced AIF nuclear translocation.

Discussion

MSCs have generated a great interest since they have potential use in regenerative medicine and tissue engineering. Both preclinical and clinical studies illustrate the

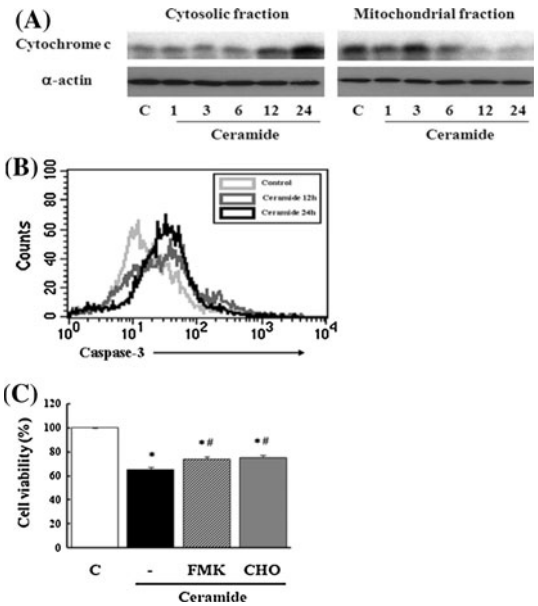

Fig. 5 Effect of ceramide on cytochrome c release and caspase activation. **a** hASCs were treated with 50 μM ceramide for indicated times. Cytosolic and mitochondrial fractions were prepared, and cytochrome c levels were determined by Western blot analysis as described under "Materials and methods". α-Actin was used as a loading control. **b** hASCs were treated with 50 μM ceramide for 12 and 24 h, and caspase-3 activation was estimated by flow cytometric analysis. **c** Effect of caspase inhibitors on ceramide-induced cell death. hASCs were treated with 50 μM ceramide for 24 h in the presence or absence of 10 μM Z-VAD-FMK (FMK) or 10 μM DEVD-CHO (CHO). Cell viability was measured by MTT assay. Data are the mean ± SEM of three independent experiments performed in duplicate. $*P < 0.05$ compared to control; $P < 0.05$ compared to ceramide alone

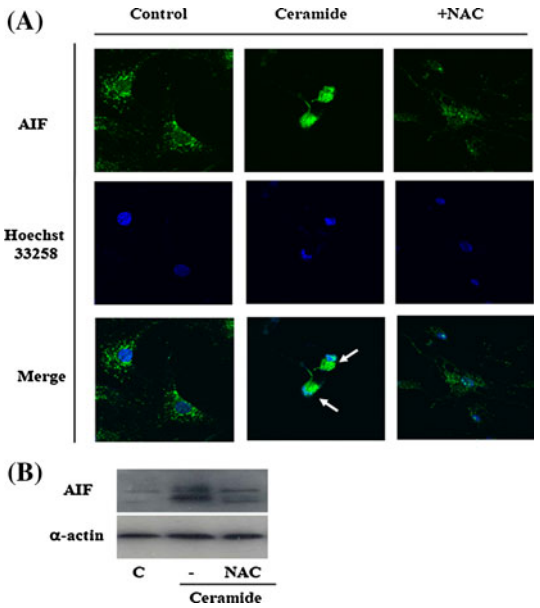

Fig. 6 Effect of ceramide on AIF nuclear translocation. **a** hASCs were treated with 50 μM ceramide for 24 h in the presence or absence of 1 mM *N*-acetylcysteine (NAC). Nuclei were counterstained with Hoechst 33258. *Arrows* indicate AIF nuclear translocation. **b** hASCs were treated with 50 μM ceramide for 24 h in the presence or absence of 1 mM *N*-acetylcysteine (NAC). Nuclear fractions were prepared, and AIF levels were determined by Western blot analysis. α-Actin was used as a loading control

therapeutic value of MSCs (Barry and Murphy 2004). Although studies demonstrating safety and effectiveness of MSC therapy have been extensively carried out, little information is available on the underlying mechanism of action and toxicology studies to demonstrate the long-term safety of these therapies (Jeon et al. 2005). Apoptosis of MSCs may lead to retardation of repair of damaged tissues.

Ceramide has been reported to induce cell death through multiple signaling mechanisms in many cell types (Richter and Ghafourifar 1999; Takai et al. 2005). However, the effect of ceramide in hASCs has not been explored yet. The present study was carried out to determine the apoptotic effect of ceramide and the underlying mechanism in hASCs.

ROS play an important role in the regulation of various functional signals involved in proliferation, apoptosis, and changes in cellular function (Kim et al. 2008, 2009; Kwon et al. 2009). The present study also showed that ceramide generates ROS and disrupts ΔΨm at early time point and that cell death was prevented by the antioxidant NAC (Fig. 3), suggesting that ROS generation is involved in the ceramide-induced cell death. Sources of ROS generated by various agents have been known to be associated with activation of NADPH oxidase in the damage of cell membrane, Ca^{2+} releases through endoplasmic reticulum (ER) stress, and the damage of mitochondria (Malhotra and Kaufman 2007). Ceramide induces ROS generation through inhibition of the mitochondrial electron transport chain in rat hepatocytes (García-Ruiz et al. 1997), human myeloid leukemia U937 cells (Quillet-Mary et al. 1997), and HL-60 cells (Gudz et al. 1997). However, the source of ROS induced by ceramide in hASCs remains to be defined.

Mitochondria play an important role in both apoptotic and necrotic cell death (Kroemer et al. 1998). The present study showed that ceramide induces a disruption of ΔΨm and causes the release of cytochrome c into the cytosol, leading to caspase activation (Figs. 4 and 5). However, the ceramide-induced cell death was partially prevented by caspase inhibitors. These results suggest involvement of a caspase-independent apoptotic mechanism in the ceramide-induced cell death. AIF plays an important role in caspase-independent cell death in many cell types (Cande et al. 2002). Therefore, we examined involvement of AIF nuclear translocation in the ceramide-induced cell death. These data are consistent with reports showing ceramide induces both cytochrome c release and AIF release from

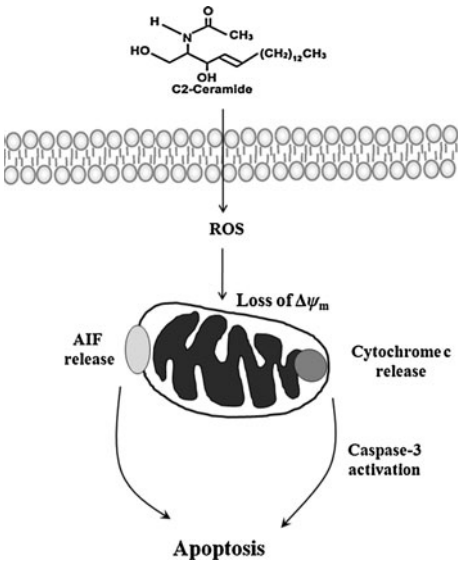

Fig. 7 A model of ceramide-induced cell death in hASCs. Treatment of ceramide caused ROS generation accompanied by disruption of mitochondrial membrane potential. Ceramide induced cytochrome c release into cytosol from mitochondria and caspase activation. In addition, ceramide caused AIF release from mitochondria and nuclear translocation. ROS generation acts upstream of both events

mitochondria in rat heart (Di Paola et al. 2004) and cortical neuronal cultures (Movsesyan et al. 2004). Previous studies also show that ceramide induces apoptosis through AIF translocation in human neuroblastoma cell line (Kim et al. 2007).

Although our data clearly show that ROS generation and AIF translocation mediate the ceramide-induced apoptosis in hASCs, it is not clear whether the AIF translocation resulted from ROS generation. Therefore, we determined the role of ROS generation in the ceramide-induced AIF translocation. The results of the present study show that the AIF translocation was blocked by the antioxidant NAC (Fig. 6), suggesting that ceramide induces a caspase-independent apoptosis through AIF nuclear translocation mediated by ROS generation in hASCs.

In conclusion, the present study shows that ceramide caused cytochrome c release from mitochondria and caspase activation. However, the ceramide-induced cell death was partially prevented by caspase inhibitors. Ceramide induced AIF release from mitochondria and nuclear translocation. Both events were inhibited by antioxidant. These data suggest that ceramide induces a caspase-dependent and caspase-independent apoptosis mediated by ROS generation in hASCs (Fig. 7).

Acknowledgments This work was supported for 2 years by Pusan National University Research Grant.

References

Barry FP, Murphy JM (2004) Mesencymal stem cells: clinical applications and biological characterization. Int J Biochem Cell Biol 36:568–584

Bieberich E, Mackinnin S, Silva J, Noggle S, Condie BG (2003) Regulation of cell death in mitotic neural progenitor cells by asymmetric distribution of prostate apoptosis response 4 (PAR-4) and simultaneous elevation of endogenous ceramide. J Cell Biol 162:469–479

Bieberich E, Silva J, Wang G, Krishnamurthy K, Condie BG (2004) Selective apoptosis of pluripotent mouse and human stem cells by novel ceramide analogues prevents teratoma formation and enriches for neural precursors in ES cell-derived neural transplants. J Cell Biol 167:723–734

Cande C, Cohen I, Daugas E, Ravagnan L, Larochette N, Zamzami N, Kroemer G (2002) Apoptosis-inducing factor (AIF): a novel caspase-independent death effector released from mitochondria. Biochimie 84:215–222

Cohen GM (1997) Caspases: the executioners of apoptosis. Biochem J 326:1–16

Colombaini L, Garcia-Gil M (2004) Sphingolipid metabolites in neural signalling and function. Brain Res Rev 46:328–355

Cuvillier O (2002) Sphingosine in apoptosis signaling. Biochem Biophys Acta 1585:153–162

De Ugarte DA, Morizono K, Elbarbary A, Alfonso Z, Zuk PA, Zhu M, Dragoo JL, Ashjian P, Thomas B, Benhaim P, Chen I, Fraser J, Hedrick MH (2003) Comparison of multi-lineage cells from human adipose tissue and bone marrow. Cells Tissues Organs 174:101–109

Denizot F, Lang R (1986) Rapid colorimetric assay for cell growth and survival. Modifications to the tetrazolium dye procedure giving improved sensitivity and reliability. J Immunol Methods 89:271–277

Di Paola M, Zaccagnino P, Montedoro G, Cocco T, Lorusso M (2004) Ceramide induces release of pro-apoptotic proteins from mitochondria by either a $Ca2^{+}$ -dependent or a $Ca2^{+}$ -independent mechanism. J Bioenerg Biomembr 36:165–170

Futerman AH, Hannun YA (2004) The complex life of simple spingolipids. EMBO Rep 5:777–782

García-Ruiz C, Colell A, Marí M, Morales A, Fernández-Checa JC (1997) Direct effect of ceramide on the mitochondrial electron transport chain leads to generation of reactive oxygen species. Role of mitochondrial glutathione. J Biol Chem 272:11369–11377

Gudz TI, Tserng KY, Hoppel CL (1997) Direct inhibition of mitochondrial respiratory chain complex III by cell-permeable ceramide. J Biol Chem 272:24154–24158

Hannun YA, Obeid LM (2002) The ceramide-centric universe of lipid-mediated cell regulation: stress encounters of the lipid kind. J Biol Chem 277:25847–25850

Jeon ES, Kang YJ, Song HY, Woo JS, Jung JS, Kim YK, Kim JH (2005) Role of MEK-ERK pathway in sphingosylphosphorylcholine-induced cell death in human adipose tissue-derived mesenchymal stem cells. Biochim Biophys Acta 1734:25–33

Kim YJ, Bae YC, Suh KT, Jung JS (2006) Quercetin, a flavonoid, inhibits proliferation and increase osteogenic differentiation in human adipose stromal cells. Biochem Pharmacol 72:1268–1278

Kim NH, Kim K, Park WS, Son HS, Bae Y (2007) PKB/Akt inhibits ceramide-induced apoptosis in neuroblastoma cells by blocking apoptosis-inducing factor (AIF) translocation. J Cell Biochem 102:1160–1170

Kim HK, Kim YJ, Kim JT, Kwon CH, Kim YK, Bae YC, Kim DH, Jung JS (2008) Alterations in the proangiogenic functions of adipose tissue-derived stromal cells isolated from diabetic rats. Stem Cells Dev 17:669–680

Kim KW, Choi CH, Kim TH, Kwon CH, Woo JS, Kim YK (2009) Silibinin inhibits plioma cell proliferation via $Ca2^{+}$/ROS/MAPK-dependent mechanism in vitro and glioma tumor growth in vivo. Neurochem Res 34:1479–1490

Kroemer G, Dallaporta B, Resche-Rigon M (1998) The mitochondrial death/life regulator in apoptosis and necrosis. Annu Rev Physiol 60:619–642

Kwon CH, Park JY, Kim TH, Woo JS, Kim YK (2009) Ciglitazone induces apoptosis via activation of p38 MAPK and AIF nuclear translocation mediated by reactive oxygen species and Ca(2+) in opossum kidney cells. Toxicology 257:1–9

Lee RH, Kim B, Choi I, Kim H, Chio HS, Suh K, Bae YC, Jung JS (2004) Characterization and expression analysis of mesenchymal stem cells from human bone marrow and adipose tissue. Cell Physiol Biochem 14:311–324

Malhotra JD, Kaufman RJ (2007) Endoplasmic reticulum stress and oxidative stress: a vicious cycle or a double-edged sword? Antioxid Redox Signal 9:2277–2293

Movsesyan VA, Stoica BA, Yakovlev AG, Knoblach SM, Lea PM IV, Cernak I, Vink R, Faden AI (2004) Anandamide-induced cell death in primary neuronal cultures: role of calpain and caspase pathways. Cell Death Differ 11:1121–1132

Murphy JM, Dixon K, Beck S, Fabian D, Feldman A, Barry F (2002) Reduced chondrogenic and adipogenic activity of mesenchymal stem cells from patients with advanced osteoarthritis. Arthritis Rheum 46:704–713

Pastorino JG, Chen ST, Tafani M, Snyder JW, Farber JL (1998) The overexpression of Bax produces cell death upon induction of the mitochondrial permeability transition. J Biol Chem 273:7770–7775

Quillet-Mary A, Jaffrézou JP, Mansat V, Bordier C, Naval J, Laurent G (1997) Implication of mitochondrial hydrogen peroxide generation in ceramide-induced apoptosis. J Biol Chem 272:21388–21395

Richter C, Ghafourifar P (1999) Ceramide induces cytochrome c release from isolated mitochondria. Biochem Soc Symp 66:27–31

Rodríguez JP, Ríos S, Fernández M, Santibañez JF (2004) Differential activation of ERK1, 2 MAP kinase signaling pathway in mesenchymal stem cell from control and osteoporotic postmenopausal women. J Cell Biochem 92:745–754

Rosse T, Olivier R, Monney L, Rager M, Conus S, Fellay I, Jansen B, Borner C (1998) Bcl-2 prolongs cell survival after Bax-induced release of cytochrome c. Nature 391:496–499

Short B, Brouard N, Occhiodoro-Scott T, Ramakrishnan A, Simmons PJ (2003) Mesenchymal stem cells. Arch Med Res 34:565–571

Takai N, Ueda T, Kawano Y, Nishida M, Nasu K, Narahara H (2005) C2-ceramide exhibits antiproliferative activity and potently induces apoptosis in endometrial carcinoma. Oncol Rep 14:1287–1291

Woodcock J (2006) Sphingosine and ceramide signaling in apoptosis. IUBMB Life 58:462–466